ACS APPLIED MATERIALS & INTERFACES

Letter

www.acsami.org

Fabrication of Well-Defined Mushroom-Shaped Structures for Biomimetic Dry Adhesive by Conventional Photolithography and Molding

Yue Wang, Hong Hu, Jinyou Shao,* and Yucheng Ding*

Micro- and Nano-manufacturing Research Center, State Key Laboratory for Manufacturing Systems Engineering, Xi'an Jiaotong University, 28 Xianning Road, Xi'an 710049, People's Republic of China

Supporting Information

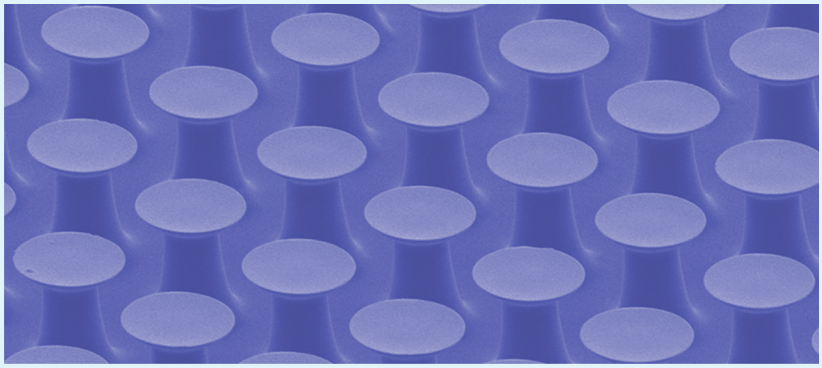

ABSTRACT: Biomimetic dry adhesives have many attractive features, such as reversible and repeatable adhesion against various surfaces. This paper presents a method for the simple fabrication of biomimetic dry adhesives composed of a mushroom-shaped structure, which is based on conventional photolithography and molding. Firstly a masked and a maskless exposure are performed on the top and bottom of a photoresist, respectively, that generates microholes with an undercut after development. This structured photoresist is then used for molding, leading to mushroom-shaped structural features after sacrificing the photoresist. Because of the convenience of photolithography, the proposed method has the potential to fabricate various dry adhesives cost-efficiently.

KEYWORDS: *mushroom-shaped, dry adhesives, photolithography, molding*

INTRODUCTION

Biomimetic dry adhesives have many applications because they can provide strong, yet reversible attachment, and repeatable adhesion property against various surfaces. Many researchers have confirmed that some small animals, such as geckos, can adhere firmly to various surfaces by van der Waals forces due to the unique topography of their feet, which consists of abundant microscopic foot hairs (setae) split into numerous nanoscale ends (spatula).[1−3] A large amount of research has been focused on various bottom-up and top-down approaches to characterize the structural shapes of dry adhesives.[4−15] According to the contact splitting theory, the dry adhesion property can be improved by decreasing the pillar diameter and increasing the number of pillars.[16] Recent theoretical and experimental research has proven that the tip shape of the pillars is a significant factor for enhancing the adhesion, and that pillars with a mushroom-shaped tip tend to be able to produce a higher pull-off force than those with concave, spherical or flat tips.[17−22] In addition, hierarchical structures have been studied to enhance the dry adhesion on surfaces with varying degrees of roughness and orientations as they improve the compliance and adaptability with regards to non-planar surfaces.[6,8,23,24] Furthermore, gecko feet were found to demonstrate excellent directional adhesion, which allows for smart attachment to and detachment from various surfaces.[9,25,26] Researchers have confirmed that tilted pillars can mimic this anisotropic adhesion, as such a microstructure can produce a strong adhesion only when loaded in a specific direction.[27,28] Therefore, to better mimic this smart adhesion, researchers have incorporated various tilted structures into artificial dry adhesives.[8,9,29]

So far, numerous processes have been proposed to fabricate different types of dry adhesives with mushroom-shaped tips. In some of these processes, the first step is to generate a mold array that has undercut microholes. For example, a mold with undercut microholes was generated by photolithography on a UV photoresist to define the microhole array and then a DUV (deep UV) exposure on a DUV sensitive material (PMGI) was

Received: November 20, 2013
Accepted: February 14, 2014
Published: February 14, 2014

   dx.doi.org/10.1021/am4052393 | ACS Appl. Mater. Interfaces 2014, 6, 2213−2218

performed to form the undercut; this involved two chemical developments because two photo-sensitive materials were used.[7] On the basis of the deep-UV patterning of commercial acrylic with semi-collimated light available from germicidal lamps and careful combination with processing conditions, relatively high-aspect-ratio fibers with overhanging caps were produced over large areas. However, this technology requires the molding and demolding to be performed twice, which increases the fabrication complexity.[30] Mushroom-shaped tips can also be generated by mechanical pressing. For example, in a two-step process proposed by Jeong,[13] a partially cured micropillar array was generated by molding a UV-curable resin first, then a modification of the micropillar tips was performed by a mechanical pressing, followed by a post-curing stage. Similarly, mushroom-shaped tips were also formed by dipping the pre-formed pillar tips into a liquid polymer and then pressing them onto a planar substrate with a constant load, following by curing at room temperature for 24 h.[9] These mechanical pressing processes can be faced with a problem related to controlling the lateral shape and spatial consistencies of the tips over a large area because of a lack of lateral confinement for the material reflow.

To fabricate an array of slanting pillars, a mold was generated via a slanting etching on poly-Si to form tilted holes with undercuts by inserting an etch-stop layer of silicon dioxide.[8] While this process is powerful for generating a tilted pillar array with spatular tips by molding, the deep ion reactive etching and tilted etching technique tends to be costly. By shearing a partially cured PDMS replica at a predetermined shear distance, a PDMS replica mold with tilted cylindrical holes and tips was achieved after being fully cured in its sheared state at 75 °C for 24 h, which resulted in a PU-based dry adhesive once it was peeled off from the PDMS replica. This technology is easy and scalable, but mushroom-shaped tips have been ignored.[26] Recently, 3D direct laser writing has been used to fabricate mushroom-shaped structures.[12] Though direct laser writing is a very flexible and rapid prototyping method, allowing the fabrication of arbitrary structures, it can have poor productivity.

This paper presents a facile method for fabricating mushroom-shaped structures based on conventional photolithography and molding. Masked and maskless exposures are performed on the top and bottom of a positive-tone photoresist on a glass substrate, respectively, that generates an array of microholes with a bottom undercut after development, followed by molding to fabricate mushroom-shaped structures. Performed on a nanopatterned substrate, it can form a hierarchical mushroom-shaped structure, whereas, when exposed with an inclined angle, slanting mushroom-shaped structures can be generated for anisotropic adhesion. It is possible to use this method for the cost-efficient fabrication of a range of mushroom-shaped adhesion structures on a large area.

EXPERIMENTAL METHODS

The basic fabrication procedure for mushroom-shaped micro pillars is shown in Figure 1. An AZ P4620 photoresist is spun on the glass slide at 1000 rpm, followed by 5 min of soft baking at 100 °C. The spin-coating and soft baking are performed twice to produce a 30 μm thick film, as measured using the Profile system. Then, a UV light is passed through a mask from the top side and the exposure dosage is adjusted to ensure a complete exposure of the photoresist. In addition, the UV light irradiates the back side and the AZ P4620 is exposed for a short time without any masking so that only a thin layer is completely exposed. Furthermore, areas in closer proximity to the substrate are better exposed. This step is simple yet significant when finally

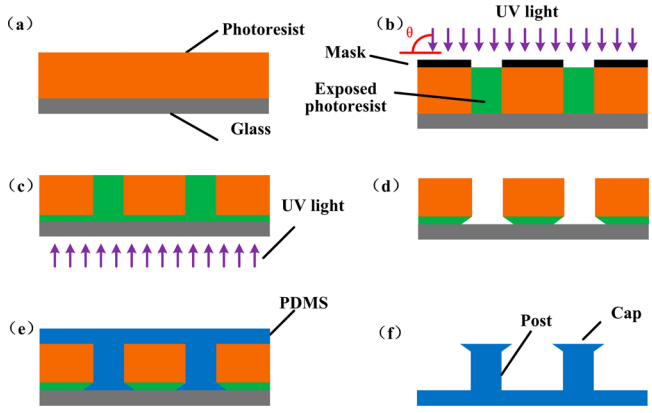

Figure 1. Schematic diagram of the processing steps for fabrication of mushroom-shaped micropillars. (a) Photoresist spin-coating and baking. (b) Photoresist exposed from top side with a mask present. (c) Flooding exposure from substrate side without any mask. (d) Photoresist is developed, leaving undercut holes. (e) Sylgard 184 is mixed then poured on the mold and cured. (f) The cured silicone is demolded, leading to mushroom-shaped pillars.

achieving the undercut microholes because the bottom of photoresist can be developed off after exposure. Following this, a precise development of the wafer is performed in a solution of 0.5 wt % NaOH. Afterwards, PDMS (Sylgard 184, Dow Chemicals) of a good replication capability and low cost is used as a filling material to duplicate the structures from the template. First, PDMS is mixed at a mass ratio of 10:1 for the pre-polymer to catalyze and degassed for 15 min under a vacuum. It is then poured on the template and degassed again under vacuum for 20 minutes. Following this, the PDMS is cured for 10 h at 60°C. As cured, the PDMS does not dissolve in ethyl alcohol, but the photoresist does, PDMS pillars with mushroom-shaped tips can be easily obtained in ethyl alcohol. In fact, this process could be used to duplicate structures with various liquid polymer materials because the photoresist will be chemically sacrificed during demolding. Therefore, after exposure to the top and back sides as well as development and molding, mushroom-shaped micropillars are produced.

Vertical Mushroom-Shaped Structure. Cap diameter is a significant parameter in dry adhesion.[17,19,21] In this process, the substrate side exposure dosage and development time are two important factors influencing the cap diameter. In our experiment, a mask with arrayed holes with a radius of 7.5 μm and the center distance of 30 μm is taken to fabricate arrayed mushroom-shaped pillars. The photoresist with a thickness of about 30 μm is exposed to 150 seconds of G-line UV light at a power of 12.5 mJ cm^{-2} from the top side with the mask. The substrate side exposure dose is one of the most important parameters influencing the cap diameter. In this process, the photoresist is dosed with 60, 120, and 180 mJ cm^{-2} from the substrate side (the transmittance property of the substrate side is shown in the Supporting Information Figure S1). Following exposure, the development time, which is another important influencing parameter for determining the cap diameter, varies from 80 to 130 s in a 0.5 wt % NaOH solution. With different development times and substrate side exposure dosages, different cap diameters can be achieved. Figure 2a shows the relationship between the cap diameter, development time and substrate side exposure dosage. Observing from the abscissa, the cap diameter becomes larger with increasing development time. In fact, the cap size is related to both the center distance of neighboring pillars and their diameter, but determined by the development time. Viewing from the vertical axis, the thickness of the exposed photoresist at the bottom is expanded, and more of the photoresist would be developed off when the substrate side exposure dose is raised. Therefore, to achieve a certain cap diameter, the development time must be decreased, and this also leads to thicker

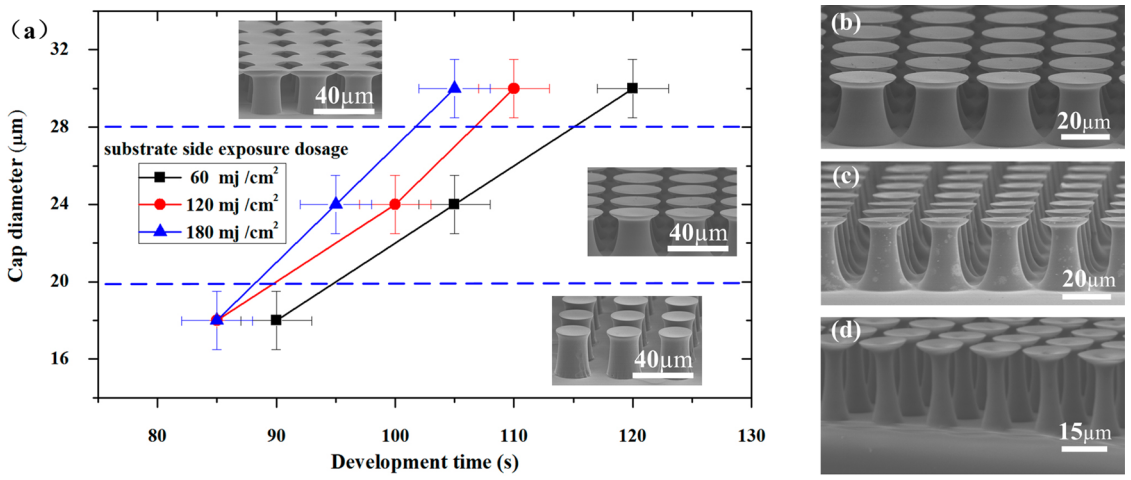

Figure 2. (a) Relationship between cap diameter, substrate side exposure dosage, and development time. The inset shows SEM images of different cap geometries. (b–d) SEM images of mushroom-shaped pillars with different aspect ratios: (b) 2:1, (c) 3:1, and (d) 6:1.

caps. In Figure 2a, using a substrate side exposure dose of 60 mJ•cm^{-2} as an example, the SEM images show three different cap geometries.

The aspect ratio of the pillars is another important factor for adhesion.[28,31] On the premise of avoiding fracture of structures, a large pillar height (therefore a large aspect ratio) is desirable for increasing the adhesion because high aspect ratio contributes to a higher elastic energy dissipated at pull-off, which can achieve higher adhesion strength.[31] Different aspect ratios of mushroom-shaped pillars can be achieved by changing the pillar height (i.e. photoresist thickness) or the pillar diameter. On spin coating, an AZ P4620 photoresist with a high viscosity is capable of producing a film that can attain a thickness of 15–18 μm at 1000 r/min or even reach 100μm through multiple coating and soft bake processes. Generally, the resolution limit of this photoresist is about 5 μm and the aspect ratio of the patterns can reach 5–10. Although the side wall verticality and aspect ratio can be improved by optimizing the various process conditions, i.e., exposure dosage, soft bake time, development time, etc., it is not easy to fabricate structures with a high aspect ratio (>10:1) and strong vertical wall. In the experiment presented here, two spin coatings at 1000 r/min were performed to give a thickness of around 30 μm. Taking arrayed holes of different diameters (15, 10, and 5 μm) as masks, mushroom-shaped pillars with three different aspect ratios are achieved as shown in Figure 2b–d.

This process can also be performed on a nano-patterned substrate, leading to a hierarchical structure with nanopillars positioned on the top of mushroom-shaped pillars. At first, a SU8 2002 photoresist is spun on the substrate followed by a two-step soft baking process. A silicon stamp with nano pillars is pressed onto the substrate to drive the negative duplication of the pattern on to the SU8 photoresist at 90 °C. After demolding, the SU8 template with arrayed nano-holes is obtained on the substrate, to provide the second level structure. Then the SU8 photoresist is exposed to UV light, followed by a two-step post-exposure baking. This method allows the SU8 template to be used repeatedly after exposure and post exposure baking since SU8 is a highly cross-linked epoxy, which is extremely difficult to remove with a conventional solvent such as sodium hydroxide or ethyl alcohol. After introducing a SU8 template on the substrate, the remaining fabrication process for a dual-level hierarchical structure is identical to that presented in Figure 1 (see the Supporting Information, Figure S2).

Figure 3a shows the SEM images of the vertical, dual-level hierarchical structures. The cap and post have diameters of 30 and 15 μm, respectively. The height and diameter of the nano hairs on the micro pillars are about 1μm and 500 nm respectively. During the demolding step, it is not easy to fabricate the nanohairs due to a lateral collapse of the high aspect-ratio structures. As mentioned above, PDMS of good replication capability is used as a filling material. However, PDMS with a low elasticity modulus is not well-suited for high-aspect-ratio nano patterning. In this experiment, both PDMS and

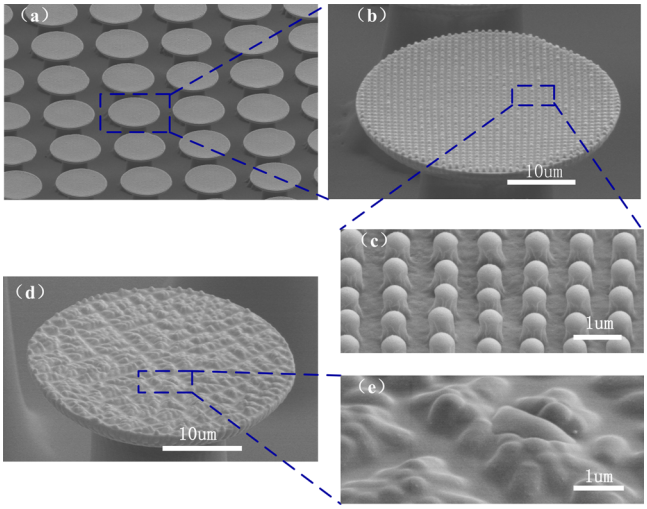

Figure 3. (a) SEM images of the vertical, dual-level hierarchical structure made from NOA81 and (b, c) its magnified image. (d) SEM images of intact PDMS micro pillars and (e) its magnified image with tangled PDMS nano pillars.

UV curable polymer NOA81 (Norland optical adhesive) are used to fabricate dual-level hierarchical structures. As a result, the micropillars can be patterned well, but the high-aspect-ratio nanohairs cannot be fabricated using the PDMS with a low elasticity modulus, as shown in Figure 3d. Meanwhile, cured NOA81 with a high elasticity modulus is rigid enough to fabricate nanoscale structures.

Research on the collapse of mushroom-shaped structures has rarely been reported, but some theoretical works on pillars have been presented.[10,32,33] On the basis of a quantitative model of lateral collapse,[34] the maximum height of the polymer for a given elastic modulus, size, and surface energy is given by the following equation

$$h_{max} = \left(\frac{\pi^4 E^* r}{2^{11}\gamma_s}\right)^{1/12}\left(\frac{12Er^3w^2}{\gamma_s}\right)^{1/4} \quad (1)$$

where $E^* = E/(1-\upsilon^2)$ is the plane strain fibril modulus, E the elastic modulus of a pillar, υ is Poisson's ratio, r is the radius of the pillar, γ_s is the surface energy and w is half the distance between neighboring pillars. According to Eeq 1, the maximum height of the micropillars (r = 7.5 μm, w = 7.5μm) for PDMS ($E \approx 2$ MPa, $\gamma_s \approx 22$ mJ m^{-2}, $\upsilon \approx 0.5$)[34,35] is about 70μm, but the maximum height of the nanohairs (r = 250 nm, w = 250 nm) is only 1μm. As shown in Figure 3d, although the PDMS micro pillars possess mushroom-shaped ends, the height of

dx.doi.org/10.1021/am4052393 | ACS Appl. Mater. Interfaces 2014, 6, 2213–2218

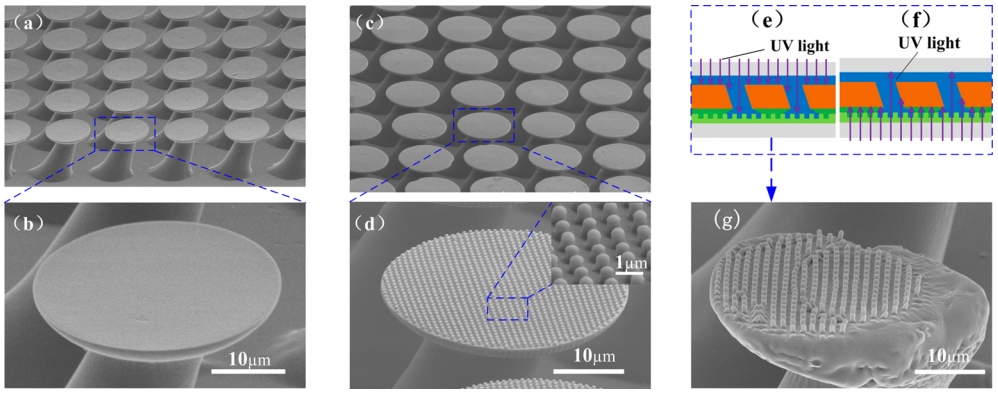

Figure 4. (a, b) SEM images of tilted micro pillars and (c, d) hierarchical structures. NOA81 cured with UV light from the (e) top side and (f) substrate side, and (g) SEM image of incompletely cured hierarchical structure.

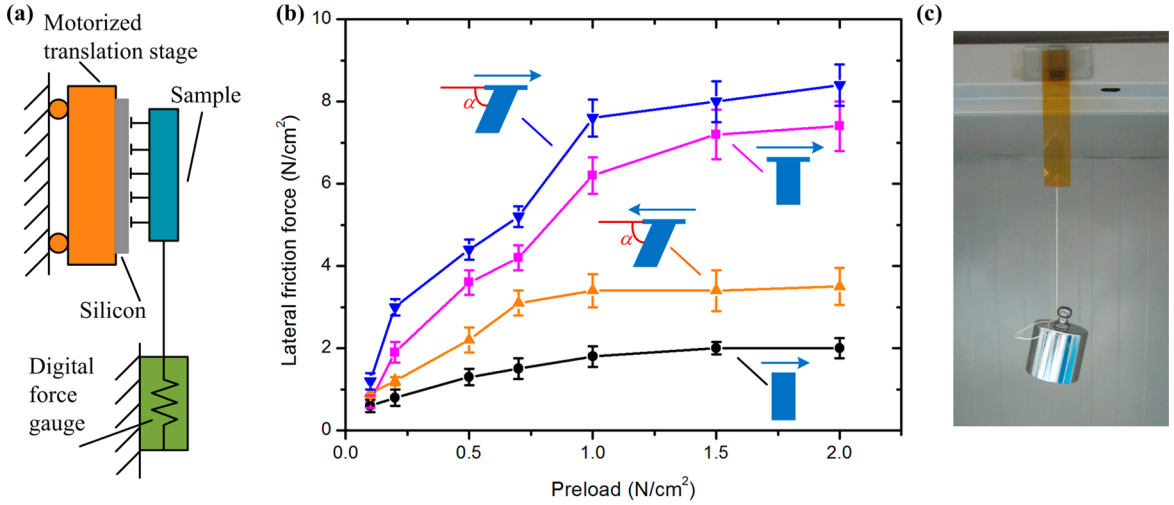

Figure 5. (a) Schematic illustration of the adhesion test set-up. (b) Adhesion performances of vertical and slanting pillars of mushroom-shaped tips as well as vertical pillars without caps. The arrows illustrate the adhesion test direction for the dry adhesives. (c) Image of a 500 g weight suspended via the pillars with mushroom-shaped tips over an area of 1 cm^2.

the post is only about 30 μm, which is much less than the maximum height of 70μm and the PDMS micro mushroom-shaped pillars remain intact. On the contrary, as shown in Figure 3e, the height of the nanopillars is about 1.0μm, which is the maximum height; and therefore, the PDMS nano pillars are tangled. Compared to the elasticity modulus of PDMS (~2 MPa), that of the UV curable polymer NOA81 (~1360 MPa) is higher. Therefore, it is adequate for fabrication of nanoscale structures of high aspect ratio without a self-matting problem, as shown in Figure 3c.

Tilted Mushroom-Shaped Structure. A slanting structure is an important factor for anisotropic dry adhesives, and here we present a convenient method to fabricate a tilted mushroom-shaped structure. As shown in Figure 1, the UV light passes through the mask at a special angle θ during the top side exposure. When θ is equal to 90°, the structures achieved are vertically oriented. When θ is less than 90°, slanting structures are generated. Therefore, it is easy to obtain a slanting structure and control the tilt angle by inclining the substrate during exposure from the top side. Once the top side has been exposed, the process then follows the information presented in Figure 1 (the dependency of the tilting angle on the irradiation angle is shown in the Supporting Information, Figure S3.)

Images a and c in Figure 4 show SEM images of tilted mushroom-shaped micro pillars and the hierarchical structures. The tilt angle can be easily adjusted by changes in the angle between the incident UV light and the substrate. Though NOA81 has a high elasticity modulus and is suitable for fabricating high aspect ratio nanoscale structures, it needs to be cured through exposure to UV light. Images e and f in Figure 4 illustrate the process of curing NOA81. At first, as shown in Figure 4e, UV light passes through NOA81 from the top side. As the NOA81 pillars and their mushroom-shaped ends are inclined the surrounding photoresist absorbs a portion of the UV light. As a result, NOA81 cannot be thoroughly solidified. Figure 4g shows a SEM image of incomplete solidified of NOA81 pillars, whose cap is fragmentary because of incomplete irradiation when exposed to 60 s of UV light at a power density of 12.5 mw cm^{-2} only from the top side. If the irradiation time is increased then NOA81 can be fully solidified, but this is not a reliable method of fabrication nor is it cost-effective. As shown in Figure 4f, if the UV light passes through NOA81 from only the substrate side, some UV light is also absorbed by the surrounding photoresist, whereas the top and substrate side UV light is complementary to each other, and together they can make NOA81 completely solidified. The perfect tilted, mushroom-shaped NOA81 structures, shown in Figure 4d, are fabricated after irradiation by UV light twice, from the top and substrate sides.

Adhesion Test. To characterize the adhesion properties of biomimetic dry adhesives fabricated using the method presented here, several biomimetic dry adhesive surfaces made of UV curable polymer NOA81 over an area of 1 cm^2 were used as test samples. Firstly, the vertical pillars tested have a diameter of 15μm and the center distance between them is 30 μm. The cap diameter is about 25μm and the total height of the pillars is approximately 30μm. To demonstrate that the mushroom-shaped tips increase adhesion strength, pillars with and without caps, of identical total height and diameter in the post part, were used as test objects to perform a

dx.doi.org/10.1021/am4052393 | ACS Appl. Mater. Interfaces 2014, 6, 2213−2218

comparison of the lateral friction force. In addition, tilted structures are important for mimicking the gecko feet at the performance in directional adhesion. The tilted pillars of the mushroom-shaped tips having the same structure parameters as the vertical pillars except for the tilt angle (~60°) were also tested to confirm that the anisotropic adhesion property can benefit from slanting structures.

Measurements of the lateral friction forces for the vertical and tilted pillars were recorded against a flat Si surface with home-built equipment, as shown in Figure 5a. This instrument primarily consists of a digital force gauge with a resolution ratio of 0.1N, a motorized translation stage (PI GmbH M-531.DD) with a high resolution of 0.1 μm and a force loading device to provide normal preload. During the adhesion test, no external normal load was applied and the stage moved at a constant rate of 10um/s until pull-off. Figure 5b shows the lateral friction forces against the preloaded value for both the vertical and tilted pillars. The lateral friction force of mushroom-shaped pillars (vertical or tilted) increases with increasing preloads due to the increased tip contact areas, and it reached a saturation level after the mushroom-shaped pillars came into complete contact with the Si surface. On the contrary, the lateral friction forces showed a small increase with the increasing preload for the pillars without caps and the values were relatively low in comparison to the mushroom-shaped pillars, which demonstrated that the mushroom-shaped tips can effectively enhance the adhesion properties. To demonstrate the practical application of this technology, a 1 cm^2 section of the vertical mushroom-shaped pillars was used to suspend a 500g counterweight. (As shown in Figure 5c, the photo was taken at 5 min after loading.)

For the tilted pillars, the maximum lateral friction force reached to ~8.4 N/cm^2 on average following the direction of the inclined angle and the force reduced to ~3.5 N/cm^2 on average in the reverse direction, suggesting that the tilted dry adhesives presented here can be used to achieve directional adhesion with the ratio to 2.4 between the forward and reverse directions, and this directional adhesion property can be explained by a peeling model. According to the Kendall peeling model, the relationship between the critical peel-off force and the peel-off angle can be given by[36]

$$\left(\frac{F}{b}\right)^2 \frac{1}{2Ed} + \left(\frac{F}{b}\right)(1 - \cos\alpha) - R = 0 \quad (2)$$

where F is the peeling force, E is the elastic modulus, b is the width of the sample, R is the energy required to fracture, and α is the peeling angle. For a single tilted pillar, b is the diameter of the cap and α is the angle between the cap and the post as shown in Figure 5b. Because of the initial leaning angle of the tilted pillar being reduced from 60° to 0° when it is pulled along the inclination angle the peel-off force is increased. However, when the pillar is pulled in the reverse direction, the peeling angle increases from 60 to 90°, and thus the peel-off force is reduced according to eq 2. Accordingly, the peel-off force of vertical pillars is less than the force of tilted pillars when pulled along the inclination angle and greater when pulled against the inclination angle. Although the maximum lateral friction force is approximately 8.4 N/cm^2, which is near to the gecko foot hairs' adhesion strength (~10 N/cm^2), the preload of this biomimetic dry adhesive's surface (>1 N/cm^2) is far larger than a gecko's (<0.01 N/cm^2), mainly because of its high aspect ratio structures.[28] In addition, the mushroom-shaped pillars are intact after several repeated peeling-off since the biomimetic dry adhesive is detachable by overcoming the interface van der Waals force, which demonstrates the biomimetic dry adhesives can be used repeatedly.

CONCLUSION

This paper has presented a convenient method for the fabrication of various biomimetic dry adhesives composed of a mushroom-shaped arrayed structure based on conventional photolithography and molding. Two exposures, one on the top and one on the bottom of a photoresist, are performed to generate an array of mushroom-shaped structures after development and molding. It is possible to exert effective control of the aspect ratio by altering the height of the pillar (i.e. the photoresist thickness) and control of the cap diameter by changing the development times. Several influencing factors, such as the material's elastic modulus and curable methods, have also been analyzed to successfully produce vertical and tilted hierarchical structures. In addition, the adhesion properties have been demonstrated using vertical and slanting mushroom-shaped micro pillars as well as vertical pillars without caps as the test samples. The mushroom-shaped tips can effectively enhance the adhesion properties and the anisotropic adhesion property can benefit from the slanting structures. The convenient, yet robust approach presented here would be highly useful for the development of various biomimetic dry adhesives in a cost-effective and fast manner.

ASSOCIATED CONTENT

Supporting Information

Schematic diagram of the processing steps for fabrication of dual-level hierarchical structure, the transmittance property of glass slide and the dependency of the tilting angle on the irradiation angle. This material is available free of charge via the Internet at http://pubs.acs.org.

AUTHOR INFORMATION

Corresponding Authors

*E-mail: jyshao@mail.xjtu.edu.cn.
*E-mail: ycding@mail.xjtu.edu.cn.

Notes

The authors declare no competing financial interest.

ACKNOWLEDGMENTS

This research was partially financed by the Major Research Program of NSFC on Nanomanufacturing (Grant 90923040), and Funds of NSFC (Grant 51005178 and 51175417)

REFERENCES

(1) Autumn, K.; Liang, Y. A.; Hsieh, S. T.; Zesch, W.; Chan, W. P.; Kenny, T. W.; Fearing, R.; Full, R. J. *Nature* **2000**, *405*, 681−685.
(2) Autumn, K.; Sitti, M.; Liang, Y.; Peattie, A. M.; Hansen, W. R.; Sponberg, S.; Kenny, T. W.; Fearing, R.; Israelachvili, J. N.; Full, R. J. *Proc. Natl. Acad. Sci. U.S.A.* **2002**, *99*, 12252−12256.
(3) Autumn, K.; Peattie, A. M. *Integr. Comp. Biol.* **2002**, *42*, 1081−1090.
(4) Jeong, H. E.; Lee, S. H.; Kim, P.; Suh, K. Y. *Nano Lett.* **2006**, *6*, 1508−1513.
(5) Geim, A. K.; Dubonos, S. V.; Grigorieva, I. V.; Novoselov, K. S.; Zhukov, A. A.; Shapoval, S. Y. *Nat. Mater.* **2003**, *2*, 461−463.
(6) Greiner, C.; Arzt, E.; Del Campo, A. *Adv. Mater.* **2009**, *21*, 479−482.
(7) Sameoto, D.; Menon, C. *J. Micromech. Microeng.* **2009**, *19*, 115002.
(8) Jeong, H. E.; Lee, J. K.; Kim, H. N.; Moon, S. H.; Suh, K. Y. *Proc. Natl. Acad. Sci. U.S.A* **2009**, *106*, 5639−5644.
(9) Murphy, M. P.; Aksak, B.; Sitti, M. *Small* **2009**, *5*, 170−175.
(10) Chandra, D.; Yang, S.; Soshinsky, A. A.; Gambogi, R. J. *ACS Appl. Mater. Interfaces* **2009**, *1*, 1698−1704.
(11) Kwak, M. K.; Jeong, H. E.; Bae, W. G.; Jung, H. S.; Suh, K. Y. *Small* **2011**, *7*, 2296−2300.
(12) Rohrig, M.; Thiel, M.; Worgull, M.; Holscher, H. *Small* **2012**, *8*, 3009−3015.
(13) Jeong, H. E.; Suh, K. Y. *Soft Matter* **2012**, *8*, 5375−5380.
(14) Bae, W. G.; Kwak, M. K.; Jeong, H. E.; Pang, C.; Jeong, H.; Suh, K. Y. *Soft Matter* **2013**, *9*, 1422−1427.
(15) Zhou, M.; Tian, Y.; Sameoto, D.; Zhang, X. J.; Meng, Y. G.; Wen, S. Z. *ACS Appl. Mater. Interfaces* **2013**, *5*, 10137−10144.

(16) Arzt, E.; Gorb, S.; Spolenak, R. *Proc. Natl. Acad. Sci. U.S.A.* **2003**, *100*, 10603−10606.
(17) Del Campo, A.; Greiner, C.; Arzt, E. *Langmuir* **2007**, *23*, 10235−10243.
(18) Kim, S.; Sitti, M.; Hui, C. Y.; Long, R.; Jagota, A. *Appl. Phys. Lett.* **2007**, *91*, 161905.
(19) Kim, S.; Aksak, B.; Sitti, M. *Appl. Phys. Lett* **2007**, *91*, 221913.
(20) Del Campo, A.; Greiner, C.; Alvarez, I.; Arzt, E. *Adv. Mater.* **2007**, *19*, 1973−1977.
(21) Kim, S.; Sitti, M. *Appl. Phys. Lett* **2006**, *89*, 261911.
(22) Carbone, G.; Pierro, E. *Small* **2012**, *8*, 1449−1454.
(23) Murphy, M. P.; Kim, S.; Sitti, M. *ACS Appl. Mater. Interfaces* **2009**, *1*, 849−855.
(24) Qu, L. T.; Dai, L. M.; Stone, M.; Xia, Z. H.; Wang, Z. L. *Science* **2008**, *322*, 238−242.
(25) Zhao, B. X.; Pesika, N.; Rosenberg, K.; Tian, Y.; Zeng, H. B.; McGuiggan, P.; Autumn, K.; Israelachvili, J. *Langmuir* **2008**, *24*, 1517−1524.
(26) Jin, K.; Tian, Y.; Erickson, J. S.; Puthoff, J.; Autumn, K.; Pesika, N. S. *Langmuir* **2012**, *28*, 5737−5742.
(27) Autumn, K.; Dittmore, A.; Santos, D.; Spenko, M.; Cutkosky, M. *J. Exp. Biol.* **2006**, *209*, 3569−3579.
(28) Jeong, H. E.; Suh, K. Y. *Nano Taday* **2009**, *4*, 335−346.
(29) Kwak, M. K.; Pang, C.; Jeong, H.; Kim, H.; Yoon, H.; Jung, H.; Suh, K. *Adv. Funct. Mater.* **2011**, *21*, 3606−3616.
(30) Sameoto, D.; Menon, C. *J. Micromech. Microeng.* **2010**, *20*, 115037.
(31) Greiner, C.; Del Campo, A.; Arzt, E. *Langmuir* **2007**, *23*, 3495−3502.
(32) Gao, H. J.; Yao, H. M. *Proc. Natl. Acad. Sci. U.S.A.* **2004**, *101*, 7851−7856.
(33) Yao, H.; Gao, H. *J. Mech. Phys. Solids* **2006**, *54*, 1120−1146.
(34) Glassmaker, N. J.; Jagota, A.; Hui, C. Y.; Kim, J. *J. R. Soc. Interface* **2004**, *1*, 23−33.
(35) Zheng, Cui, *Nanofabrication Principles, Capabilities and Limits*; Springer: New York, 2008; Chapter 6, pp 197−198.
(36) Kendall, K. *J. Phys. D: Appl. Phys.* **1975**, *8*, 1449−1452.